Gradient Catastrophe and Fermi Edge Resonances in Fermi Gas

E. Bettelheim,[1] Y.Kaplan,[1] and P. Wiegmann[2]

[1] *Racah Institute of Physics, Hebrew University, Jerusalem, Israel*
[2] *The James Franck Institute, University of Chicago*

A smooth spatial disturbance of the Fermi surface in a Fermi gas inevitably becomes sharp. This phenomenon, called *the gradient catastrophe*, causes the breakdown of a Fermi sea to disconnected parts with multiple Fermi points. We study how the gradient catastrophe effects probing the Fermi system via a Fermi edge singularity measurement. We show that the gradient catastrophe transforms the single-peaked Fermi-edge singularity of the tunneling (or absorption) spectrum to a set of multiple asymmetric singular resonances. Also we gave a mathematical formulation of FES as a matrix Riemann-Hilbert problem.

1. Introduction The FES (Fermi edge singularity [1–3]) observed in absorption of X-rays in metals more than 70 years ago as a power law peak at the Fermi-surface, is one of the most prominent and well understood quantum many-body phenomena caused solely by Fermi statistics.

FES also has been demonstrated in tunneling experiments [4–7]: a sudden switch-on of a contact potential due to a change in the capacity of the contact in tunneling causes a power law in tunneling current vs the bias voltage: $I(V) \sim V^{-2a+ka^2}$ [8]. Here $\delta = \pi a$ is a scattering phase of the ensuing potential and k is the number of scattering channels. In the case of an attractive potential ($a > 0$) the current peaks at the Fermi edge.

The physics of the FES is explained by the phenomena of Orthogonal Catastrophe [10]: the state of a Fermi gas $\langle\Omega'|$ after a suddenly imposed a localized potential is almost orthogonal to a state of the unperturbed Fermi gas $|\Omega\rangle$. Their overlap vanishes with a level spacing Δ as a power law $\langle\Omega'|\Omega\rangle \sim (\Delta/E_F)^{ka^2}$.

FES acquires new features out of equilibrium, where a *gradient catastrophe* takes place. A gradient catastrophe is a hydrodynamic instability observed in many classical (and, recently, in quantum atomic) systems. In Ref. [9] it has been shown that a gradient catastrophe also takes place in a Fermi gas. The ballistic propagation of macroscopical packets and fronts in Fermi gases inevitably enters a gradient catastrophe regime, where the initially smooth fronts develop large gradients and undergo a shock wave phenomenon: packets overturn as shown in Fig 1. This phenomena shows up differently in different quantum observables. Ref. [9] discusses the Orthogonality Catastrophe [10] in a non-staionary regime: the overlap of the state of a shaken-up Fermi gas with a propagating packet (both before and after the shock). In this paper we study FES. We show that shock waves cause additional resonance peaks (see Fig. 2). Observation may not be easy since electronic times are too short, but does not seem impossible. From the theoretical viewpoint FES in a non-stationary regime reveals important (and new) aspects of the Orthogonality Catastrophe. Both catastrophes are caused solely by Fermi statistics.

In a related work [11] FES has been studied in a steady out-of-equilibrium settings with a two-steps Fermi distribution (see also [12]). The two steps show up as two FES
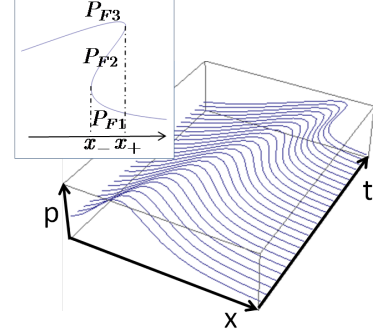

FIG. 1: Time progression of the Fermi edge. The front overhangs, giving rise to three Fermi (see inset) edges ($P_{F3} > P_{F2} > P_{F1}$) between the trailing (x_-) and leading (x_+) edges.

peaks occur - one for each of the Fermi edge. Our setting is different. We discuss FES in a non-stationary, time dependent phenomenon.

2. Tunneling in a non-stationary regime. We consider the following situation:
(i) A Fermi gas is in contact with a localized resonant level (a quantum dot). It is initially uncharged and provides no scattering to electrons. When an electron tunnels to the dot, it suddenly charges the dot, switching-on a small potential $H \to H' = H + U$ localized at the dot, such that $|a| < 1/2$ [8]. We assume no further interaction, no dissipation, ignore spin and channels.
(ii) A semiclassical electronic front or a packet - a state with a spatially inhomogeneous density matrix ϱ has been
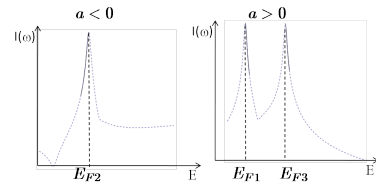

FIG. 2: A schematic plot of tunneling current for $a < 0$ (left panel) and $a > 0$ (right panel), solid lines show computed power law asymptotes. Dashed lines interpolate between resonances. $a < 0$ displays a single peak after the shock, while $a > 0$ displays two peaks.

initially created in a Fermi gas as is in Ref.[9] and Fig. 1. The state evolves before the shake-up as $e^{iHt}\varrho e^{-iHt}$.

E.g., a smooth potential well (namely, of spatial extent much larger than the Fermi length) centered away from the dot is applied to the Fermi gas. A large number of electrons is trapped in the well. Then the well is suddenly removed. The electronic packet propagates towards the dot, eventually hits it, facilitating tunneling. Alternatively, we may consider two conductors with different chemical potentials suddenly brought into contact. The conductor with smaller chemical potential is in contact with a dot. A front of electronic density propagates toward the smaller chemical potential of the dot.

This situation is described by a density matrix $|\Omega\rangle\langle\Omega|$, where

$$|\Omega\rangle = \exp\left(\frac{i}{\hbar}\int P_0(x)\varphi(x)dx\right)|0\rangle$$

is a Fermi coherent state, $|0\rangle$ is the ground state of a Fermi gas with a Fermi momentum $P_F > 0$, and $0 < P_0(x) \ll P_F$ is an initial momenta of a packet. The field φ is a chiral canonical Bose field related to the chiral part of electronic density

$$\varphi(x) = \hbar\sum_{k\neq 0}\frac{1}{k}e^{\frac{i}{\hbar}kx}\rho_k, \quad \rho_k = \sum_{p>0}c_p^\dagger c_{p+k}, \qquad (1)$$

where p and $p + k$ are electronic momenta close to the Fermi momentum P_F. We assume that $P_0(x)$ is smooth on the Fermi length scale $\hbar|\nabla P_0|/P_0 \gg P_F$. This condition justifies the semiclassical analysis described below.

The tunneling current is given by the golden rule [1, 8]. In units of a tunneling amplitude $I(\omega)|_{\hbar\omega=eV+E_F}$ reads

$$I(\omega, t) \propto \text{Re}\int_0^\infty e^{i\omega\tau}G(t+\frac{\tau}{2}, t-\frac{\tau}{2})d\tau, \qquad (2)$$

$$G(t_1, t_2) = \langle\Omega|e^{iHt_2}ce^{iH'(t_1-t_2)}c^\dagger e^{-iHt_1}|\Omega\rangle \qquad (3)$$

Here $c = \sum_k e^{-ikx_0}c_k$ and x_0 is the position of the dot.

Since all the physics is concentrated at the Fermi edge a knowledge of the dispersion at the edge is sufficient

$$\epsilon_p = E_F + v_F(p - P_F) + \frac{(p - P_F)^2}{2m} + \dots. \qquad (4)$$

In the literature the parabolic part of the dispersion is routinely ignored. In that case our effect disappears [13].

We evaluate $G(t_1, t_2)$ in the regime when a typical time of tunneling $\tau = t_2 - t_1 > 0$ is much less than the time it takes for a packet to change. This approximation does not allow us to compute the broadening of the resonance at a frequency range $\gamma \sim v_F(\nabla P_0/\hbar)^{1/2}$, but it captures the power law shoulders of resonances.

Under this assumption during the short time of tunneling the energy dependence of the Fermi velocity and scattering phase δ caused by potential U can be dropped in some interval $|\epsilon - E_F| \ll \Lambda$ at the Fermi edge, where the cut-off Λ (typically of the Fermi scale) is assumed to be larger than $v_F P_0$ and $\hbar/\tau$. This amounts a shift of energy levels after scattering downwards by a constant amount a (in units of level spacing): $\epsilon_p \rightarrow \epsilon_p - a$.

In Ref. [14] it has been shown that the vertex operator $e^{a\varphi}$ implements a shift of momenta such that a perturbed Hamiltonian and perturbed states are $H' = e^{-a\varphi(x_0)}He^{a\varphi(x_0)}$ and $|\Omega'\rangle = e^{a\varphi(x_0)}|\Omega\rangle$. Then Green's function reads

$$G(t_1, t_2) = \langle\Omega|c(t_2)e^{-a\varphi(x_0,t_2)}e^{a\varphi(x_0,t_1)}c^\dagger(t_1)|\Omega\rangle. \quad (5)$$

This formula is standard. The only difference is that the density matrix does not commute with the Hamiltonian and therefore the process is not-stationary.

3. Gradient Catastrophe: Riemann equation for Fermi Gas. We demonstrate the gradient catastrophe on the evolution of the Wigner function - a simpler object than (3). The Wigner function describes occupation in phase space:

$$n_F(x, p, t) = \int\langle\Omega|c^\dagger(x+\frac{y}{2}, t)c(x-\frac{y}{2}, t)|\Omega\rangle e^{\frac{ipy}{\hbar}}dy \quad (6)$$

We assume that the front is plane or radial, such that the dynamics is essentially one dimensional and chiral.

Semiclassically, the Wigner function is equal to 1 in a bounded domain $p < P_F(x, t)$ of the phase space (p, x) - the Fermi sea - and vanishes outside the Fermi sea $n_F(x, p, t) \approx \Theta(P_F(x, t) - p)$. This form is valid as long as the gradients of the spatial dependence of the Fermi momentum $P_F(x, t)$ are small. The shape of the initial Fermi surface is given by the density matrix $P_F(x, 0) = P_F + P_0(x)$.

How does the Fermi surface change in time? It does not, if one neglects dispersion of the Fermi gas, i.e., treats the velocity $v_p = d\epsilon_p/dp$ as a constant: the front translates with the Fermi velocity without changing its shape. It does change dramatic fashion if the dispersion in (4) (no matter how small) is taken into account.

The Wigner function (for a dispersion $\epsilon_p = p^2/2m$) obeys the equation

$$(\partial_t + v_p\nabla)n_F(x, p, t) = 0, \quad v_p = p/m \qquad (7)$$

The solution of this equation

$$n_F(x, p, t) = n_F(x - v_p t, p, 0) \approx \Theta(P_0(x - v_p t) - p) \quad (8)$$

shows that a moving Fermi momentum $P_F(x, t)$ obeys a *hodograph* equation

$$P_F(x, t) = P_0(x - P_F(x, t)/m \cdot t) \qquad (9)$$

This is Riemann solution of Euler's equations for hydrodynamics of a compressible one-dimensional fluid

$$\partial_t P_F + \nabla E_F = 0, \quad E_F(x, t) = P_F^2(x, t)/2m \qquad (10)$$

Riemann's equation leads to shock waves: the velocity of a point with momentum $P_F(x)$ is $P_F(x)/m$: higher parts of the front move faster. The front gets steeper, and

eventually achieves an infinite gradient – a shock at some finite time. After this moment the Riemann equation has at least three real solutions, $P_{F3}(t) > P_{F2}(t) > P_{F1}(t)$, confined between two turning points $x_-(t), x_+(t)$, the trailing and leading edges respectively (Fig.1).

This phenomena is the gradient catastrophe. Any smooth disturbance of the Fermi surface eventually arrives to a point when the Fermi surface acquires infinite gradients, and then becomes multi-valued between moving turning points $x_\pm$. We focus on that region.

5. Slowly evolving Fermi edges Away from turning points we can employ the Whitham averaging method known in the theory of non-linear waves [15]. The method has been applied to electronic systems in [9]. It is based on a separation of scales between slowly varying Fermi edges and fast oscillations of electronic states. In short, the Whitham method suggests to treat the slowly changing Fermi edges as constants while computing Green's function (3), and then to include the motion of the Fermi Edges in the final result. Motion of the Fermi edges is determined by the Riemann equation (10). This approach is valid away from turning points [16]). It can be justified mathematically using an integrable non-linear equation for Green's function obtained in [17].

6. Fermi edge resonances In the shock region $x_- < x_0 < x_+$ we must evaluate (3) over a state with three Fermi edges, where electrons occupy states below E_{F1} and between E_{F2} and E_{F3} (see Fig.3). We computed the current at a frequency close to edges $\hbar\gamma \ll \varepsilon_i (\hbar\omega - E_{Fi}) \ll v_F P_0$. In units of cut-offs it reads:

$$I(\omega) \propto |\hbar\omega - E_{Fi}|^{3a^2 - 2\varepsilon_i a} \prod_{n>m} E_{nm}^{2\varepsilon_n \varepsilon_m a^2} \prod_{j\neq i} E_{ij}^{-2\varepsilon_j a},$$

where $\varepsilon_i = (-1)^{i+1}$, $i = 1, 2, 3$ and $E_{ij} = E_{Fi} - E_{Fj}$. The Fermi energies all depend on time according to (9).

If the potential is attractive $a > 0$ (a common case) the current features a peak at E_{F1} (almost zero bias) and an additional resonance at E_{F3} with a power law to the right of the edges. Current is suppressed at the edge E_{F2}. If potential is repulsive $a < 0$ a peak appears at the edge E_{F2} with a power law to the left to the edge Fig.2.

Apart from additional resonances, a noticeable difference with a shock region is the exponent and time-dependent amplitudes. Outside of the shock region where there is only one Fermi edge or at a larger energy $|E_{Fi} - E_{Fj}| \ll |\omega - E_F| \ll \Lambda$ where the fine structure of Fermi edges becomes negligible, the current is given by a standard formula [1, 2] $I(\omega) \propto (\omega - E_F)^{a^2 - 2a}$ where only the edge E_F depends on time.

7. Bosonic representation The result could be understood using bosonic formalism. First we separate fast oscillatory modes at each edge

$$c(t, x_0) = \sum_i e^{\frac{i}{\hbar} P_{Fi} x(t)} \psi_i(t)$$

where $\psi_i(t)$ are slowly changing modes and $x(t) = x_0 - v_F t$. Then we represent slow modes through components

of the Bose field $\partial_x \varphi_i = i\psi_i^\dagger(t)\psi_i(t)$ as

$$\psi_i \propto (\varepsilon_i \prod_{j\neq i} E_{ij}^{\varepsilon_j})^{1/2} e^{-\varepsilon_i \varphi_i}. \qquad (11)$$

The Bose field (1) is a sum of its components $\varphi = \sum_i \varphi_i$. Component of the Bose field represent particle-holes excitations close at each edge. At $v_F/\tau \gg E_{ij}$ they can be treated as independent canonical Bose fields. Their variances $C_i(t_1, t_2) = -\frac{1}{2}\langle\Omega| (\varphi_i(t_2) - \varphi_i(t_1))^2 |\Omega\rangle$ are not difficult to compute. As it follows form (1), C_1 and C_3 are sums of $(\cos\epsilon\tau - 1)/\epsilon$ over all possible energy of a particle-hole excitations provided that a particle is taken out from the first band $p < P_{F1}$ and the second band $P_{F2} < p < P_{F3}$. Similarly C_2 is the sum over momentum of a hole particle excitations provided that a hole is taken out for the a "gap" between P_{F1} and P_{F2}. For example $C_2 = \left(\sum_{\epsilon>0}^{E_{21}} - \sum_{E_{32}}^\Lambda\right)(\cos\epsilon\tau - 1)/\epsilon$. Computing these integrals at $\tau \gg \hbar/|E_{ij}|$ one obtains

$$C_i(\tau) = -\log\tau + \varepsilon_i \sum_{j\neq i} \varepsilon_j \log|E_{ij}| \qquad (12)$$

The time independent term in (12) explains the prefactor in (11): a correlator $\langle\psi_i^\dagger(t_1)\psi_i(t_2)\rangle \propto \frac{\varepsilon_i}{x(\tau)}$ must be also obtained for the Bose field as $(\prod_{j\neq i} E_{ij}^{-\varepsilon_i \varepsilon_j})e^{C_i}$.

In the Bose representation, Green's function (5) is a sum of edge components

$$G(t_1, t_2) = \sum_i (\varepsilon_i \prod_{j\neq i} E_{ij}^{-\varepsilon_i \varepsilon_j})e^{\frac{i}{\hbar} E_{Fi}\tau} G_i(t_1, t_2), \qquad (13)$$

$$G_i = \langle e^{(\varepsilon_i - a)(\varphi_i(t_2) - \varphi_i(t_1))}\rangle \prod_{j\neq i} \langle e^{-a(\varphi_j(t_2) - \varphi_j(t_1))}\rangle$$

Computing, we obtain Green's function in the form of two factors: 'closed loops' where each edge contributes equally and 'open lines' corresponding to each edge [1].

$$G = e^C \cdot L, \quad C = a^2 \sum_i C_i, \quad L = \sum_i L_i, \qquad (14)$$

$$L_i = \varepsilon_i e^{\frac{i}{\hbar} E_{Fi}\tau} \prod_{j\neq i} E_{ij}^{-\varepsilon_j \varepsilon_i} e^{(1-2\varepsilon_i a)C_i} \qquad (15)$$

This prompts our main result. Below we substantiate by formulating Riemann-Hilbert problem for FES.

8. Fredholm Determinants with integrable kernel Following [1], Green's function can be seen as two multiplicative factors $G(t_1, t_2) = e^C \cdot L$ - open lines L and closed loops $e^C = \langle\Omega|e^{-a\varphi(t_2)}e^{a\varphi(t_1)}|\Omega\rangle$. Wick's theorem gives a representation of these factors through Fredholm determinants

$$e^C = |\langle\Omega|\Omega'\rangle|^2 \det(\mathbf{1} + \mathbf{K}), \quad L = \text{tr}\left[(\mathbf{1} + \mathbf{K})^{-1}\mathbf{P}\right] \quad (16)$$

with a kernel describing particle-hole excitations [3]

$$K(p_1, p_2) = \sum_{q\in\Omega} M_{p_1, q}(t_1) M_{q, p_2}^*(t_2), \qquad (17)$$

$$P_{p_1, p_2} = M_{p_1}(t_1) M_{p_2}^*(t_2). \qquad (18)$$

Here $M_{p,q}(t) = \langle\Omega|e^{-a\phi(t)}c_p^\dagger c_q|\Omega\rangle$ and $M_p(t) = \langle\Omega|c(t_2)e^{-a\phi(t_1)}c_p^\dagger|\Omega\rangle$ are matrix elements between states where a particle-hole pair, or just one particle are added to the state $|\Omega\rangle$. The sum in (17) runs over occupied states of $|\Omega\rangle$ - a set of states denoted by Ω [18].

At $\tau \ll \hbar/E_F$ we may neglect the energy dependence of velocity such that time dependence amounts to a shift of a coordinate by $v_F t$: $x_0 \to x(t) = x_0 - v_F t$. Then $M_{pq}(t) = e^{\frac{i}{\hbar}(q-p)x(t)}\langle\Omega'|\Omega;p,q\rangle$ is an overlap between state $\langle\Omega'|$ and a particle-hole excitation of the state $|\Omega\rangle$ with momenta $p \notin \Omega$ and $q \in \Omega$. Similarly $M_p = e^{-\frac{i}{\hbar}px(t)}\langle(p;\Omega)'|\Omega;p\rangle$ is an overlap of states $|\Omega\rangle$ and a state $|\Omega'\rangle$ with an added particle with momenta p.

If $\langle p'|$ is a single particle state of the perturbed Hamiltonian and $|p\rangle$ is likewise an unperturbed state then their overlap (in units of level spacing) is $\frac{\sin(\pi a)}{\pi(p-p')}$. The formula extends to many particle states $\langle\underline{p}|$ and $|\underline{p}'\rangle$, where $\underline{p} = p_1,\ldots,p_N$ and $\underline{p}' = p_1',\ldots,p_N'$ is a Cauchy determinant $(\frac{\pi}{\sin(\pi a)})^N\langle\underline{p}|\underline{p}'\rangle = \det\frac{1}{p_i - p_j'} = \frac{\prod_{i>j}(p_i-p_j)(p_i'-p_j')}{\prod_{i,j}(p_i'-p_j)}$. With the help of this formula, the matrix elements in (17) can be computed in a manner similar to Ref. [3]:

$$M_{qp} = e^{\frac{i}{\hbar}(q-p)x(t)}\frac{r(p)s(q)}{p-q}, \quad M_p = e^{-\frac{i}{\hbar}px(t)}r(p), \qquad (19)$$

$$r(p) = \prod_i (p - P_{Fi})^{\varepsilon_i a}, \quad s(q) = \frac{\sin\pi a}{\pi}\prod_i (P_{Fi} - q)^{-\varepsilon_i a}.$$

where $p \notin \Omega$, $q \in \Omega$ are momenta of particles and holes. Also, a general Orthogonality Catastrophe formula reads

$$\langle\Omega|\Omega'\rangle = \prod_{i>j} E_{ij}^{\epsilon_i\epsilon_j a^2}. \qquad (20)$$

These formulas extend the result in [1–3] to multiple edges.

9. Fredholm equation The next step is to invert the Fredholm kernel $\mathbf{K}$. It can be done in a straightforward manner similar to [3] employing the Wiener-Hopf method at every edge. However, calculations become more structured if we use the *integrable* property of the kernel, a general property (see [19–21]) which derives from the integrable nature of free fermion correlators [17]. An integrable kernel has the form

$$K_{p,p'} = \frac{\sum_{\alpha=1}^N f_\alpha(p)g_\alpha(p')}{p-p'}, \quad \sum_{\alpha=1}^N f_\alpha(p)g_\alpha(p) = 0.$$

In our case $N = 2$, and as follows from (17,19):

$$f_1(p) = e^{-\frac{i}{\hbar}px(t_1)}r(p), \quad f_2(p) = Q(p,\tau)f_1(p), \qquad (21)$$

$$g_2(p) = e^{\frac{i}{\hbar}px(t_2)}r(p), \quad g_1(p) = -Q(p,\tau)g_2(p),$$

$$Q(p,\tau) = \int_{q\in\Omega} e^{-\frac{i}{\hbar}v_F q\tau}\frac{s^2(q)dq}{p-q}. \qquad (22)$$

Let $\vec{F} = (\mathbf{1} + \mathbf{K})^{-1}\vec{f}$ be the solution of the singular integral equation

$$\vec{F}(p) + \int_{p'\notin\Omega} K_{p,p'}\vec{F}(p')dp' = \vec{f}(p), \quad p \notin \Omega. \qquad (23)$$

Then the closed loops and open lines (16) are

$$\frac{1}{v_F}\frac{dC}{d\tau} = \text{tr}\left((\mathbf{1}+\mathbf{K})^{-1}\frac{d\mathbf{K}}{d\tau}\right) = i\int_{p\notin\Omega}(g_1 F_1 - g_2 F_2)\,dp$$

$$L = \int_{p\notin\Omega}(g_2 F_1)\,dp,$$

10. Matrix Riemann-Hilbert problem The Fredholm equation (23) is sufficient to obtain the singular behavior at Fermi edges. However, it is instructive to cast the FES problem into the matrix RH problem along the lines described in [21]. In that form FES problem falls in the general scheme of integrable problems. Also the RH-problem is the most suitable for analysis near edges [22].

A central object of the RH problem is a matrix-valued functions $m(p)$ analytic in a complex p-plane cut along the unoccupied intervals $P_{F1} < p < P_{F2}$ or $p > P_{F3}$ Fig. 3, defined such that at infinity m approaches the unit matrix, and that its boundary value on the cuts $m_\pm = m(p+i0)$ connects vector the $\vec{F}$ to the vector $\vec{f}$ as

$$\vec{F}(p) = m_+(p)\vec{f}(p), \quad p \in \Omega. \qquad (24)$$

In Ref. [21] it has been shown that the matrix is a solution of the RH-problem:

$$m_+ v = m_-, \quad v_{\alpha\beta} = \delta_{\alpha\beta} - 2\pi i f_\alpha g_\beta. \qquad (25)$$

In the case of FES

$$v(p) = \mathbf{1} + 2\pi i e^{\frac{i}{\hbar}v_F p\tau}r^2(p)\begin{pmatrix} -Q & -1 \\ Q^2 & Q \end{pmatrix}. \qquad (26)$$

Asymptotes at edges can be found by the steepest-

FIG. 3: Matrix m jumps on segments of real axis corresponding to unoccupied states of $|\Omega\rangle$ (solid line). Steepest descent contour goes vertically (dashed line) in the upper half plane.

descent method described in [22]. The steepest-descent contour starts from Fermi edges and extends to $i\infty$ in the upper half-plane as is in Fig. 3. Along this contour the rapidly falling exponential factor $e^{\frac{i}{\hbar}pv_F\tau}$ in (26) suppresses the jump of the matrix m except at small segments near the Fermi edges. Each edge equally contributes to closed loops as is in (14). The contribution of each edge to open lines comes with its own oscillatory factor and its own amplitude in accordance with (13-12).

[1] P. Nozières, C.T. De Dominicis, Phys.Rev. 178, 1097 (1969)

[2] G. D. Mahan, Phys. Rev. 163, 612 (1967)

[3] K. Ohtaka, Y. Tanabe Phys. Rev. B 30, 4235 (1984)

[4] A. K. Geim, et al., Phys. Rev. Lett. 72, 2061 (1994)

[5] D. H. Cobden, B. A. Muzykantskii, Phys. Rev. Lett. 75, 4274 (1995),

[6] I. Hapke-Wurst, et.al., Phys. Rev. B 62 12621 (2000)

[7] Yu. N. Khanin, et.al., JETP, 105, 152 (2007)

[8] K.A. Matveev, A.I. Larkin, Phys. Rev. B 46, 15337 (1992)

[9] E. Bettelheim, A. G. Abanov, P. Wiegmann, Phys. Rev. Lett. 97, 246402 (2006)

[10] P.W. Anderson, Phys. Rev. Lett. 18 1049 (1967)

[11] D.A. Abanin, L.S. Levitov, Phys.Rev.Lett. 93, 126802 (2004).

[12] D. B. Gutman, Y. Gefen, A. D. Mirlin. *ArXiv e-prints 1010.5645*, 2010.

[13] Importance of the spectrum curvature at the Fermi surface has been also emphasized in M. Pustilnik, M. Khodas, A. Kamenev, and L. I. Glazman, Phys. Rev. Lett. 96, 196405 (2006)

[14] K.D. Schotte, U. Schotte, Phys. Rev. 182,479 (1969)

[15] G. B. Whitham, Linear and nonlinear waves. John Wiley & Sons Inc., 1999

[16] At turning points where gradients are of the order of a Fermi scale enhanced quantum corrections blur Fermi edges, E. Bettelheim, P. Wiegmann, unpublished

[17] E. Bettelheim, A. G. Abanov, P. Wiegmann J. Phys. A41 (2008) 392003

[18] Formulas equivalent to (17) appeared in [3].

[19] A. R. Its, et.al., J. Mod. Phys. B , 4 1003 (1990)

[20] M. Jimbo, T. Miwa, Y. Mori, M. Sato, Physica 1D, 80 (1980)

[21] P. Deift , A. Its, X. Zhou Ann. Math., 146, 149 (1997)

[22] P. Deift , X. Zhou, Ann. Math., 137, 295 (1993)